Applied Composite Materials **11:** 33–55, 2004.

Effective Elastic and Plastic Properties of Interpenetrating Multiphase Composites

XI-QIAO FENG*, ZHI TIAN, YING-HUA LIU and SHOU-WEN YU
Department of Engineering Mechanics, Tsinghua University, Beijing 100084, China
e-mail: fengxq@tsinghua.edu.cn

(Received 3 September 2003; accepted 18 September 2003)

Abstract. In interpenetrating phase composites, there are at least two phases that are each interconnected in three dimensions, constructing a topologically continuous network throughout the microstructure. The dependence relation between the macroscopically effective properties and the microstructures of interpenetrating phase composites is investigated in this paper. The effective elastic moduli of such kind of composites cannot be calculated from conventional micromechanics methods based on Eshelby's tensor because an interpenetrating phase cannot be extracted as dispersed inclusions. Using the concept of connectivity, a micromechanical cell model is first presented to characterize the complex microstructure and stress transfer features and to estimate the effective elastic moduli of composites reinforced with either dispersed inclusions or interpenetrating networks. The Mori–Tanaka method and the iso-stress and iso-strain assumptions are adopted in an appropriate manner of combination by decomposing the unit cell into parallel and series sub-cells, rendering the calculation of effective moduli quite easy and accurate. This model is also used to determine the elastoplastic constitutive relation of interpenetrating phase composites. Several typical examples are given to illustrate the application of this method. The obtained analytical solutions for both effective elastic moduli and elastoplastic constitutive relations agree well with the finite element results and experimental data.

Key words: micromechanics, constitutive relation, effective elastic moduli, interpenetrating phase composite, finite element analysis, Mori–Tanaka method, connectivity.

1. Introduction

Recently, much attention has been attracted to interpenetrating or co-continuous phase composites, which contains at least two phases that are each interconnected in three dimensions, constructing a topologically continuous network throughout the microstructure. If any one of the constituent phases were removed from such a composite, the remaining material would form a self-supporting, open-celled foam which can still bear loading. Many biomaterials such as bones and trunks also have interpenetrating microstructures. Of late years, some methods (e.g., directed metal oxidation, self-propagating high-temperature synthesis, and gas pressure assisted infiltration) have been developed for synthesizing interpenetrating phase composites [1–12]. This new generation of composites possesses some physical

* Corresponding author.

and mechanical properties that are evidently different from and often superior to conventional fiber- or particle-reinforced composites [1, 2]. Since an interpenetrating phase is continuous in all directions, some desired aspects of its properties can be utilized more efficiently in the overall behavior of composites [1, 2, 13]. In a two-phase interpenetrating or bi-continuous composite made of metal and ceramic, for example, the ceramic phase enhances the abrasive resistance and fracture strength while the metal improves the properties of electrical conductivity and plasticity. However, how interpenetrating microstructures influence the mechanical properties of composites remains a question largely unanswered, due in large part to a scarcity of experimental data or theoretical investigation in this field.

The determination of the overall effective properties of interpenetrating multiphase composites is of great interest, but little work has been done on this subject. Micromechanical analysis of heterogeneous materials provides their overall behavior from the known properties of individual constituents (e.g., matrix and inclusions). Various estimation schemes (e.g., dilute concentration or non-interacting method, self-consistent method, generalized self-consistent method, and Mori–Tanaka method) have been proposed to calculate the effective transport moduli (e.g., thermal conductivity, electrical conductivity, elastic moduli, dielectric constants, piezoelectric coefficients, and magnetic permeability) of heterogeneous materials or composites [14–16]. However, most of the previous work has been conducted for those composite materials comprised of well-defined inclusions (e.g., spheres, whiskers, flakes and cylinders) dispersed in a connected matrix phase, because it is much more difficult to treat interpenetrating multiphase composites.

Using the concept of matricity introduced first by Poech and Ruhr [17], Leesle *et al.* [18, 19] developed a self-consistent matricity model to simulate numerically the mechanical behavior of an isotropic two-phase composite with a coarse interpenetrating microstructure. Levassort *et al.* [20] suggested a unit cell model to estimate the effective electromechanical moduli of a 3-3(3-0) piezoelectric two-phase composite. Wegner and Gibson [2] suggested a numerical model to estimate the effective properties of interpenetrating binary composites. This model was directed mainly towards simulating the mechanical properties of isotropic materials reinforced with coarse particles in such a large volume fraction that they are interconnected as a three-dimensional network. These models are difficult to characterize the complicated microstructures of interpenetrating multiphase composites, especially when the spatial distribution of individual phases and the macroscopic properties of composites are anisotropic. Using statistical correlation functions, Torquato [16, 21, 22] established the multi-point bounds for heterogeneous materials, which are sharper than the Voigt–Reuss (or one-point) bounds and the Hashin–Shtrikman (or two-point) bounds. Until recently, however, applications of high-point bounds are still very limited because of the prohibitive complexity involved in ascertaining the statistical correlation functions for engineering composites.

One of the key considerations in estimation of the effective constitutive relation of a composite is the appropriate modeling of the stress transfer relation of the

constituent phases with specific microstructures. Long fibers can bear high stresses only in their axial direction, while platelets with high diameter-to-thickness ratios can transfer stress effectively in any in-plane directions. In interpenetrating composites, however, the reinforcing phase can transfer stresses effectively in all directions. In the present paper, a micromechanical method is employed for estimating the effective elastic and plastic properties of interpenetrating multiphase composites. A cell model is defined to describe the interpenetrating microstructures including the volume fractions, connectivities, and anisotropic spatial distributions of the constituent phases. Our present attention is focused on the determination of the effective elastic moduli and elastoplastic constitutive relations of composites. Some examples are given to examine the efficiency and accuracy of this method.

2. Unit Cell Model

2.1. CHARACTERIZATION OF MICROSTRUCTURES

Many natural interpenetrating phase materials in biology (e.g., bones in mammals and the trunks and limbs of many plants) are anisotropic both in microstructure and in macroscopic behaviors [1]. Man-made interpenetrating phase composites derived by such approaches as directed metal oxidation and colloidal methods also possess somewhat anisotropic properties. However, there is still a lack of micromechanical methods for simulating the mechanical behaviors of anisotropic interpenetrating phase composites.

Now, let us consider a macroscopically homogeneous n-phase composite, in which the elastic properties and spatial arrangements of individual phases may be anisotropic. Assume that in the composite, n_1 phases (say phases $1, 2, \ldots, n_1$) are each continuously self-connected in three dimensions, and the other n_2 phases (i.e., phases $n_1+1, n_2+2, \ldots, n$ with $n_1+n_2 = n$) appear as well-defined, disconnected inclusions. If a constituent material exists both in the form of a continuous network and dispersed inclusions, then it is considered as two different phases, a self-connected or interpenetrating phase and a dispersed inclusion phase. Connectivity suggested by Newnham *et al.* [23] is a practical concept for describing the spatial arrangement of each phase in such a composite since it gives the number of dimensions in which each component is self-connected. The connectivity characterizing the microstructural feature of the above-defined n-phase composite is designated as $3_1 - 3_2 - \cdots - 3_{n_1} - 0_{n_1+1} - 0_{n_1+2} - \cdots - 0_n$, where the subscripts stand for the corresponding phases. A phase of fiber or flake shape, with connectivity being 1 and 2, respectively, can also be incorporated easily in the present model, but is omitted here for conciseness.

Choose one interpenetrating phase, say the n_1th one, as the matrix of the composite, which usually has a relatively large volume fraction. It might be assumed, for the sake of simplicity, that all the isolated inclusions of the n_2 phases are embedded in this matrix. Then the interpenetrating matrix and all the n_2 constituent phases of inclusion shape are regarded as a single hybrid phase, which is continu-

ously self-connected in three dimensions. Thus, the microstructure of the n-phase composite is simplified as an interpenetrating n_1-phase material in which all the phases are each continuously self-connected. Its connectivity can be simplified as $3_1 - 3_2 - \cdots - 3_{n_1}(3_{n_1} - 0_{n_1+1} - 0_{n_1+2} - \cdots - 0_n)$, where the expression in the parentheses indicates the microstructure of the composite matrix phase, as defined above.

2.2. UNIT CELL

For such a multiphase composite with complex, interpenetrating microstructures, a cubic cell of unit volume, filled by the n_1 interpenetrating phases, can be specified according to the volume fractions, connectivity and spatial arrangements of the phases in the composite. An interpenetrating phase is shown in Figure 1(a) [24]. An interpenetrating composite can be synthesized by filling the remaining empty part by other materials. Assume the anisotropic principal axes are aligned along the x_1-, x_2- and x_3-axes, referring to a Cartesian coordinate system $(0 - x_1x_2x_3)$. Each self-connected phase is presented in the unit cell as three mutually orthogonal branches with rectangular cross-sections, as shown in Figure 1(b). The dimensions of the three branches can be determined according to the volume fraction and anisotropic spatial distribution of this phase. The anisotropic microstructure of an interpenetrating phase, say the αth one, is described by only three size parameters, a_α, b_α and c_α, as shown in Figure 1(b). Since the cubic cell is assumed to be of unit volume, the parameters a_α, b_α and c_α are non-dimensional. This unit cell model keeps the most significant features of microstructures and stress transfer relations of interpenetrating multiphase composites. More parameters may be introduced further in the cubic cell to characterize the microstructures more exactly, but this will certainly make the numerical computation and parameter determination cumbersome.

The burgeoning development in computational techniques of image analysis and the concomitant increase in the computational speed of computers have allowed quantitative characterization of the spatial arrangement of the constituent phases in multiphase composites. Mathematically, the spatial distribution of the phases can be determined from several cross-sections of different directions, provided that the composite is statistically uniform. For a two-phase composite with the principal axes aligned in the x_1-, x_2- and x_3-directions, for example, a cross-section normal to one principal axis, say x_1, is shown in Figure 2 [9]. The cross-section fractions of the reinforcing (white) phase and the (black) matrix in this cross-section can be determined by image analysis and designated as s_{1,x_1} and $s_{2,x_1} = 1 - s_{1,x_1}$, respectively, where the first subscript of a parameter denotes the corresponding phase, and the second stands for the direction of the normal of the corresponding cross-section. Similarly, one can get s_{1,x_2}, $s_{2,x_2} = 1 - s_{1,x_2}$, s_{1,x_3} and $s_{2,x_3} = 1 - s_{1,x_3}$. For an isotropic composite, the cross-section fractions of phases are independent of the direction, that is, $s_{1,x_1} = s_{1,x_2} = s_{1,x_3}$ and $s_{2,x_1} = s_{2,x_2} = s_{2,x_3}$.

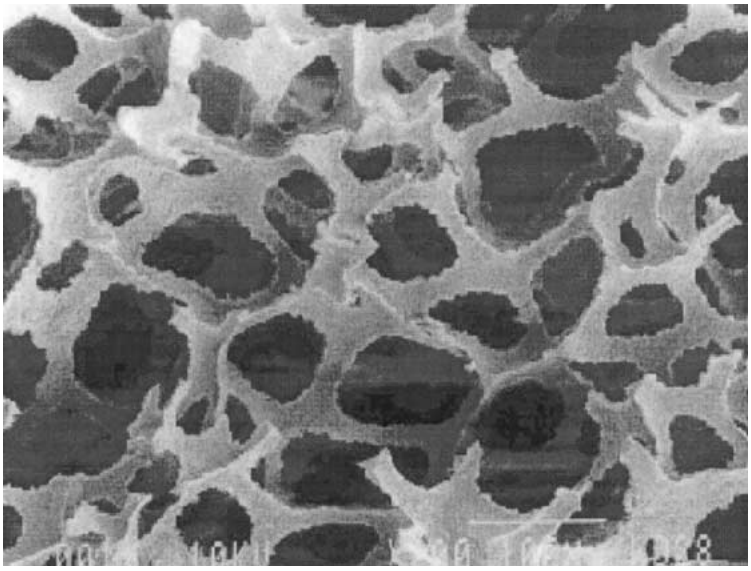

(a)

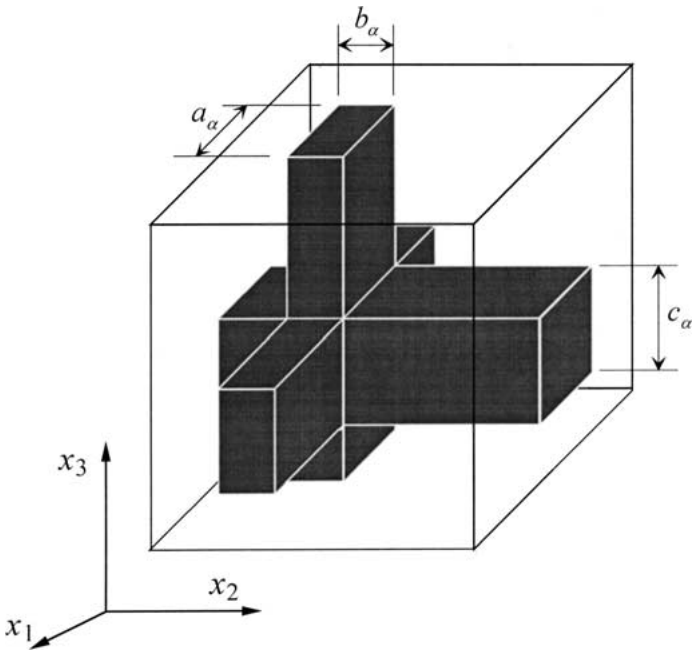

(b)

Figure 1. (a) A single interpenetrating phase in a composite [24], and (b) its model in the unit cell.

Figure 2. A cross-section of an interpenetrating two-phase composite [9].

Thus, the size parameters of the αth phase in the unit cell are related to the cross-section fractions by

$$b_\alpha c_\alpha = s_{\alpha,x_1}, \qquad a_\alpha c_\alpha = s_{\alpha,x_2}, \qquad a_\alpha b_\alpha = s_{\alpha,x_3}, \tag{1}$$

from which one obtains

$$a_\alpha = \left(\frac{s_{\alpha,x_2} s_{\alpha,x_3}}{s_{\alpha,x_1}}\right)^{1/2}, \qquad b_\alpha = \left(\frac{s_{\alpha,x_1} s_{\alpha,x_3}}{s_{\alpha,x_2}}\right)^{1/2},$$
$$c_\alpha = \left(\frac{s_{\alpha,x_1} s_{\alpha,x_2}}{s_{\alpha,x_3}}\right)^{1/2}. \tag{2}$$

The volume fraction of an interpenetrating phase is related to the three size parameters by

$$f_\alpha = a_\alpha b_\alpha + a_\alpha c_\alpha + b_\alpha c_\alpha - 2a_\alpha b_\alpha c_\alpha. \tag{3}$$

In the case of isotropic distribution, one has that $a_\alpha = b_\alpha = c_\alpha$, and then

$$f_\alpha = a_\alpha^2(3 - 2a_\alpha). \tag{4}$$

To illustrate the method for defining a unit cell, two examples are given in Figure 3, corresponding to two five-phase composites. In Figure 3(a), three phases

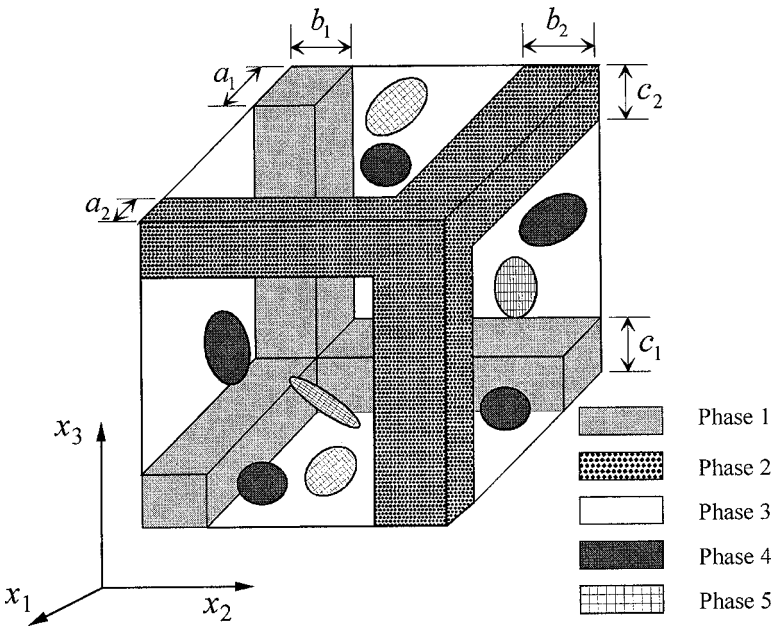

(a)

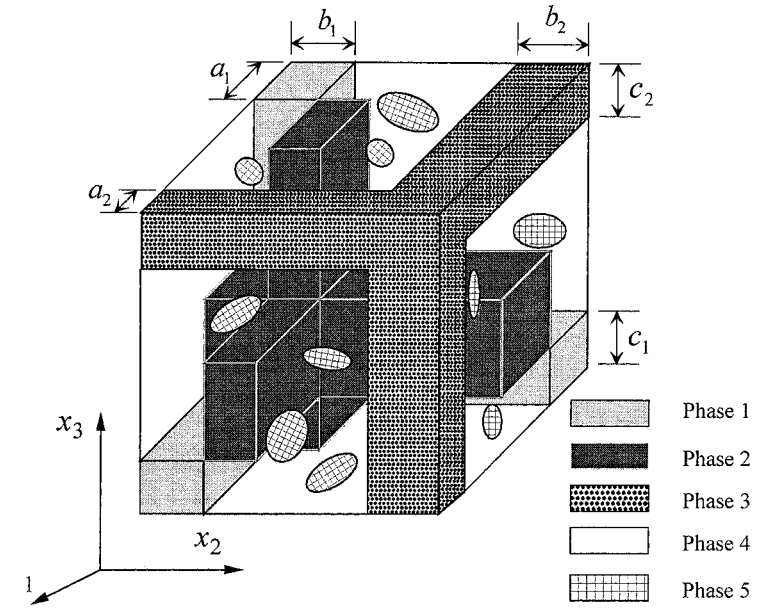

(b)

Figure 3. Unit cell models of two five-phase composites.

are self-connected in three dimensions and the other two appear as dispersed inclusions, and in Figure 3(b), four phases are self-continuous and the other is of inclusion shape. Such unit cells for multiphase composites are of interest in analysis, design and characterization of actual materials. On one hand, more than two phases are often used in a composite to get better comprehensive properties. On the other hand, if a constituent material of a composite exists in different forms (network or particles), it is convenient to consider it as different phases in the theoretical model for easier calculation, as aforementioned. In what follows, we will illustrate the construction of the unit cell model and its application in determination of the effective elastic moduli of interpenetrating-phase composites.

3. Estimation of Effective Elastic Moduli

To yield an analytical estimate on the effective elastic moduli of a composite with complicated microstructures containing both dispersed inclusions and continuously self-connected phases, some assumptions and simplifications are necessary. In this section, we determine the overall effective elastic moduli from the above-suggested unit cubic cell model via a two-step procedure.

First, we determine the effective moduli of the above-defined hybrid matrix phase, in which a self-connected phase (the n_1th one) embeds the n_2 inclusion-dispersed phases, by using one of the conventional micromechanics methods (e.g., dilute concentration method, self-consistent method, generalized self-consistent method, Mori–Tanaka method). The simplest one is the dilute concentration method, which neglects completely the interaction of inclusions. When considering interaction effects, one may estimate the effective moduli by using the self-consistent method, Mori–Tanaka method, and other such "effective medium" approaches [14–16]. In the present paper, only the Mori–Tanaka method [25] will be employed because it may easily derive the effective moduli of inclusion-dispersed composites with good accuracy even for a high volume fraction of inclusions.

The Mori–Tanaka method [25] estimates the effective moduli by assuming that each inclusion is placed in an infinite pristine matrix subjected to the average stress $\boldsymbol{\sigma}_{\mathrm{m}}$ or the average strain $\boldsymbol{\varepsilon}_{\mathrm{m}}$ in the far field. For the composite matrix with n_2 reinforcing phases in the form of differently oriented inclusions, the effective stiffness tensor $\mathbf{C}$ can be written as an analytical form

$$\mathbf{C} = \left(f_{\mathrm{m}}\mathbf{C}_{\mathrm{m}} + \sum_{\alpha=1}^{n_2} f_{\mathrm{r}\alpha} \langle \mathbf{C}_{\mathrm{r}\alpha} : \mathbf{A}_{\alpha} \rangle \right) : \left(f_{\mathrm{m}}\mathbf{I} + \sum_{\alpha=1}^{n_2} f_{\mathrm{r}\alpha} \langle \mathbf{A}_{\alpha} \rangle \right)^{-1}, \tag{5}$$

where the subscripts m and r stand for the quantities of the hybrid matrix and the reinforcing phase, respectively, α implies the αth reinforcing phase, f_{m} and $f_{\mathrm{r}\alpha}$ denote the volume fractions, and $\mathbf{C}_{\mathrm{m}}$ and $\mathbf{C}_{\mathrm{r}\alpha}$ denote the elastic stiffness tensors of the corresponding phases. A boldface letter stands for a two- or four-order tensor, and a colon between two tensors denotes contraction (inner product) over two

indices. The angle brackets $\langle\cdot\rangle$ represent the orientation average of a quantity. The fourth-order tensor $\mathbf{A}_\alpha$, which is the average strain concentration tensor, is defined by

$$\boldsymbol{\varepsilon}_{\mathrm{r}\alpha} = \mathbf{A}_\alpha : \boldsymbol{\varepsilon}_{\mathrm{m}}, \tag{6}$$

where $\boldsymbol{\varepsilon}_{\mathrm{r}\alpha}$ denotes the average strain in the αth reinforcing phase (inclusions).

The partial concentration factor A_α was given by Walpole [26] as

$$\mathbf{A}_\alpha = [\mathbf{I} + \mathbf{P}_\alpha : (\mathbf{C}_{\mathrm{r}\alpha} - \mathbf{C}_{\mathrm{m}})]^{-1}, \tag{7}$$

where the fourth-ordered tensor $\mathbf{P}_\alpha$ is related to the Eshelby's tensor $\mathbf{S}$ by the relation

$$\mathbf{P}_\alpha = \mathbf{S}_\alpha : (\mathbf{C}_{\mathrm{m}})^{-1}. \tag{8}$$

Therefore, $\mathbf{P}_\alpha$ depends on the orientation and shape of the inclusion as well as on the elastic moduli of the surrounding matrix. Some expressions of the Eshelby's tensor and the average strain-concentration tensor can be found in [27].

The second step is to estimate the effective elastic moduli of the cubic cell, either by a finite element method or by an approximate analytical method. For a composite with dispersed inclusions, the iso-stress and iso-strain assumptions lead, respectively, to the lower and upper bounds of elastic moduli. These two methods were first introduced by Reuss and Voigt, and, therefore, are also referred to as the Reuss and Voigt methods, respectively. However, neither the stresses nor the strains are uniform in the unit cell. Therefore, an appropriate combination of the iso-stress and iso-strain assumptions may yield the effective elastic moduli of the cubic cell in a manner much easier than the finite element numerical analysis. Both the analytical and numerical methods will be adopted in what follows, and it will be shown in the sequel that their results agree well.

To calculate the effective elastic moduli by using the iso-strain and iso-stress assumptions, we decompose the unit cell into series and parallel sub-cells. For isotropic composites, there are only two independent elastic constants (e.g., Young's modulus and shear modulus) in the constitutive relation, which can be determined from any direction of decomposition. For anisotropic composites, however, there are more independent elastic constants, which should be determined from sub-cell decompositions of different directions. In addition, the boundary conditions prescribed on the boundary of the unit cell play a important role in estimation of effective moduli. The periodic displacement boundary condition is more appropriate than the traction boundary condition, and, therefore, should be adopted. However, the exact periodic displacement boundary can be satisfied only by numerical iteration. Therefore, the displacement boundary condition corresponding to a uniform strain field is assumed in our analytical solution based on the iso-strain and iso-strain assumptions, while the exact periodic displacement boundary condition is used in our numerical solution.

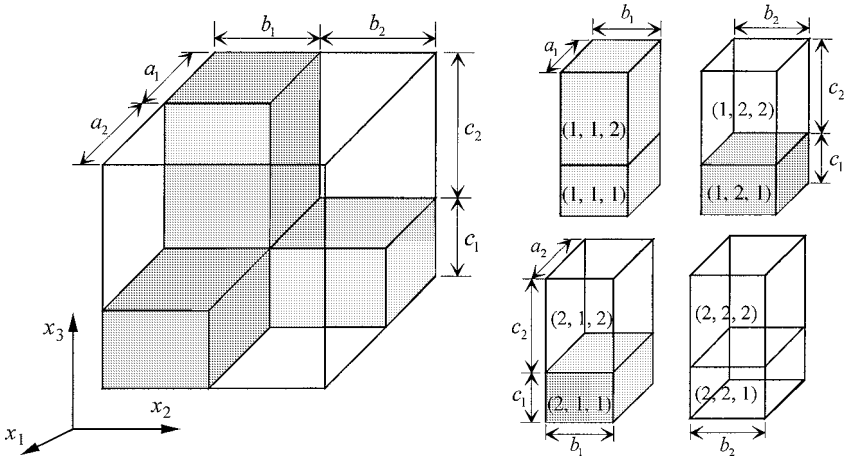

Figure 4. (a) The unit cell of an interpenetrating two-phase composite, and (b) its decomposition.

To determine the effective Young's modulus E_3 and shear moduli G_{31} and G_{32}, for example, the unit cell, consisting of n_1 self-connected phases (see, e.g., Figure 3), is divided into $n_1 \times n_1$ sub-cells parallel to the x_3-axis, each containing n_1 series blocks. The effective moduli of each sub-cell are determined from the constitutive relations (either elastic or elastoplastic) and volume fractions of its constituent phases by adopting the iso-stress assumptions. Finally, the elastic moduli of the whole cell can be calculated from the obtained constitutive property of the $n_1 \times n_1$ sub-cells by using the iso-strain assumption and the homogenization technique. Such a decomposition scheme is schematized in Figure 4 for an interpenetrating two-phase composite.

Evidently, there are three possible directions to divide the cell. If the composite is isotropic, estimates of the effective Young's modulus and shear modulus are independent of the dividing direction. For an anisotropic composite with oriented network phases, the effective elastic moduli in different directions should be derived from the corresponding decomposition direction. In the isotropic case, for example, the effective Young's modulus and shear modulus can be determined by

$$E = \sum_{\alpha=1}^{n_1}\sum_{\beta=1}^{n_1}\left\{\left[\left(\sum_{\gamma=1}^{n_1}\frac{V_{\alpha\beta\gamma}}{E_{\alpha\beta\gamma}}\right)^{-1}\sum_{\gamma=1}^{n_1}V_{\alpha\beta\gamma}\right]\sum_{\gamma=1}^{n_1}V_{\alpha\beta\gamma}\right\},$$
$$G = \sum_{\alpha=1}^{n_1}\sum_{\beta=1}^{n_1}\left\{\left[\left(\sum_{\gamma=1}^{n_1}\frac{V_{\alpha\beta\gamma}}{G_{\alpha\beta\gamma}}\right)^{-1}\sum_{\gamma=1}^{n_1}V_{\alpha\beta\gamma}\right]\sum_{\gamma=1}^{n_1}V_{\alpha\beta\gamma}\right\}, \tag{9}$$

where (α, β, γ) denotes the serial number of a sub-cell in the x_1-, x_2- and x_3-directions (Figure 4(b)), and $E_{\alpha\beta\gamma}$ and $V_{\alpha\beta\gamma}$ denote the Young's modulus and volume of the (α, β, γ) sub-cell.

4. Examples for Calculating Effective Elastic Moduli

4.1. EXAMPLE 1: CONVENTIONAL COMPOSITES REINFORCED BY DISPERSED INCLUSIONS

For a composite reinforced by distributed inclusions, only the matrix phase is self-connected in three-dimensions. Thus, the unit cell is reduced to the *representative volume element* (RVE), which is extensively employed in the micromechanics of composites. The effective moduli of the composite can be given directly from Mori–Tanaka method, i.e., from Equation (5). In this case, therefore, the present model is identical to the conventional micromechanics models.

For a binary composite reinforced by particles of spherical shape, for instance, Mori–Tanaka method yields the effective bulk modulus K and shear modulus G as

$$\begin{aligned} K &= K_{\mathrm{m}} + \frac{c_{\mathrm{r}} K_{\mathrm{m}}(K_{\mathrm{r}} - K_{\mathrm{m}})}{K_{\mathrm{m}} + \beta_1(1 - c_{\mathrm{r}})(K_{\mathrm{r}} - K_{\mathrm{m}})}, \\ G &= G_{\mathrm{m}} + \frac{c_{\mathrm{r}} G_{\mathrm{m}}(G_{\mathrm{r}} - G_{\mathrm{m}})}{G_{\mathrm{m}} + \beta_2(1 - c_{\mathrm{r}})(G_{\mathrm{r}} - G_{\mathrm{m}})}, \end{aligned} \tag{10}$$

with

$$\beta_1 = \frac{1 + \nu_{\mathrm{m}}}{3(1 - \nu_{\mathrm{m}})}, \qquad \beta_2 = \frac{2(4 - 5\nu_{\mathrm{m}})}{15(1 - \nu_{\mathrm{m}})}, \tag{11}$$

where

$$K_{\mathrm{m}} = \frac{E_{\mathrm{m}}}{3(1 - 2\nu_{\mathrm{m}})}, \qquad G_{\mathrm{m}} = \frac{E_{\mathrm{m}}}{2(1 - \nu_{\mathrm{m}})}$$

and ν_{m} are the bulk modulus, shear modulus and Poisson's ratio of the matrix, respectively, K_{r} and G_{r} are the bulk modulus and shear modulus of the reinforcing phase.

4.2. EXAMPLE 2: AN INTERPENETRATING TWO-PHASE COMPOSITE

For an interpenetrating binary composite, the effective moduli can be estimated easily from the unit cubic cell in Figure 4 by adopting the combination of iso-tress and iso-strain assumptions. This simple case is of great significance in engineering. For illustration, we assume that both the phases are isotropic, elastic and uniformly distributed in all directions. For such a case, one has that $a_1 = b_1 = c_1 = a$, $a_2 = b_2 = c_2 = 1 - a$ and the volume fraction of the reinforcing phase $f_1 = 3a^2 - 2a^3$.

Table I. Material constants of the constituent phases.

Material	Young's modulus E (GPa)	Shear modulus G (GPa)	Yield stress σ^{s} (MPa)	Strain-hardening exponent n
420 stainless	210	81.4	1432.62	13.8
150P bronze	110	41.35	135.96	7.8125
Alumina	380	141.26		

Then, the effective Young's modulus E and shear modulus G are derived in the following explicit form:

$$E = a^2 E_{\mathrm{r}} + (1-a)^2 E_{\mathrm{m}} + 2a(1-a)\left(\frac{a}{E_{\mathrm{r}}} + \frac{1-a}{E_{\mathrm{m}}}\right)^{-1},$$
$$G = a^2 G_{\mathrm{r}} + (1-a)^2 G_{\mathrm{m}} + 2a(1-a)\left(\frac{a}{G_{\mathrm{r}}} + \frac{1-a}{G_{\mathrm{m}}}\right)^{-1}, \tag{12}$$

which are functions merely of the volume fraction of the reinforcing phase via the relation $f_1 = 3a^2 - 2a^3$, though the effects of the interpenetrating microstructure have been included.

To examine the accuracy of the above method based on the decomposition of series and parallel sub-cells, the commercial finite element program ABAQUS-6.2.1 is used to calculate the effective elastic moduli of the unit cell in Figure 4(a). The periodic displacement boundary conditions are prescribed on the unit cell [28]. A bi-continuous composite made of 420 stainless steel and 150P bronze is taken as an example. The Young's moduli and shear moduli of the two phases are given in Table I. The analytical solution in Equation (12), the finite element results and the experimental results of Wegner and Gibson [2] are shown in Figure 5. Evidently, the approximate analytical method based on sub-cell decomposition agrees very well with the numerical method and the experimental results.

4.3. EXAMPLE 3: INTERPENETRATING THREE-PHASE COMPOSITES

Now we consider a composite consisting of three-phases, each of which constructs a three-dimensional network [16]. The unit cell is shown in Figure 6. Assume that all the three phases are isotropic. Without loss of generality, phase 2 is taken as the matrix. By decomposing the unit cell into series and parallel sub-cells and using the iso-strain and iso-stress assumptions, the effective Young's modulus E and the effective shear modulus G are derived as

$$E = a^2 E_1 + (1-a-b)^2 E_2 + b^2 E_3 + \frac{2a(1-a-b)E_1 E_2}{(1-a)E_1 + aE_2} + \frac{2b(1-a-b)E_2 E_3}{bE_2 + (1-b)E_3} + \frac{2abE_1 E_2 E_3}{bE_1 E_2 + (1-a)E_1 E_3 + aE_2 E_3},$$

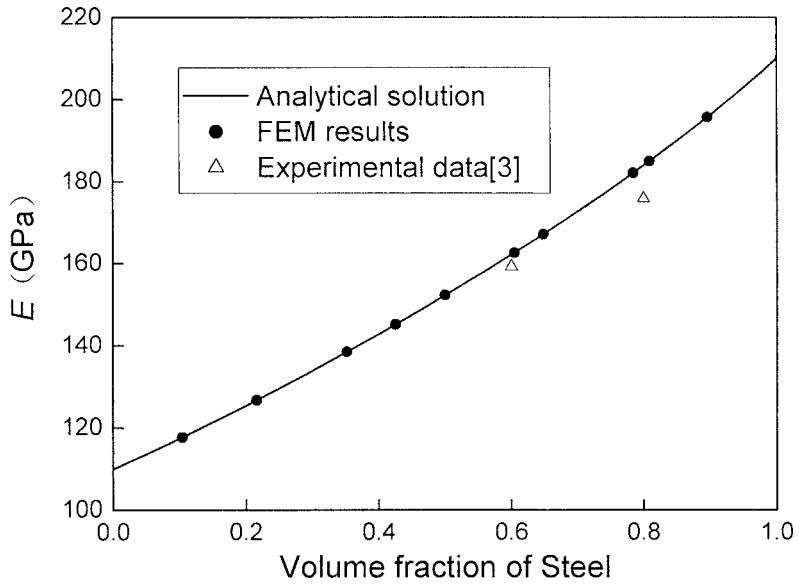

(a)

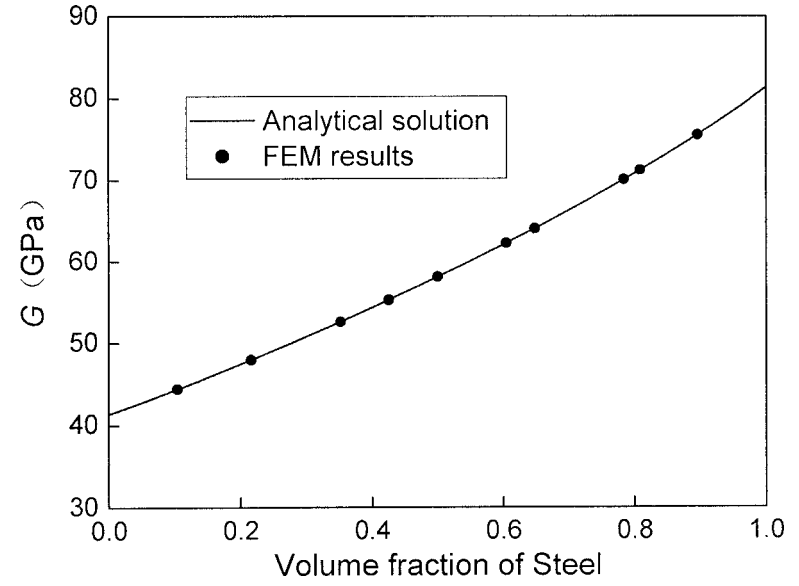

(b)

Figure 5. Effective elastic moduli of the co-continuous stainless steel/bronze composite: (a) Young's modulus, and (b) shear modulus.

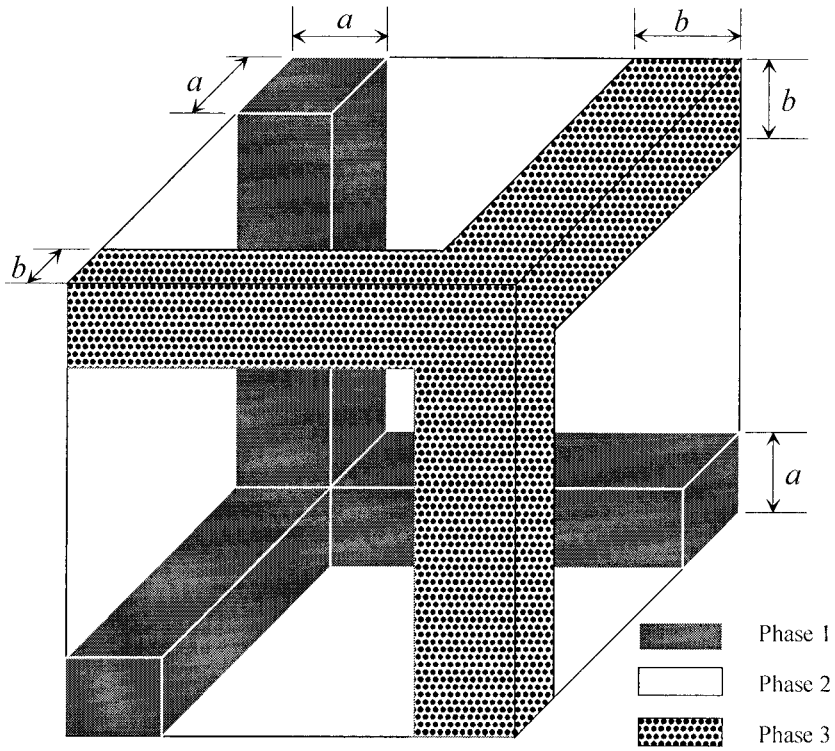

Figure 6. The unit cell of an interpenetrating three-phase composite.

$$G = a^2G_1 + (1-a-b)^2G_2 + b^2G_3 + \frac{2a(1-a-b)G_1G_2}{(1-a)G_1 + aG_2} + \frac{2b(1-a-b)G_2G_3}{bG_2 + (1-b)G_3} + \frac{2abG_1G_2G_3}{bG_1G_2 + (1-a)G_1G_3 + aG_2G_3}, \tag{13}$$

where E_α and G_α denotes the Young's modulus and shear modulus of the αth phase, respectively, a and b are the dimensionless parameters related to the volume fraction of phases 1 and 3, as shown in Figure 6.

To verify the accuracy of the analytical solution in Equation (13), numerical calculations of finite element method are also performed by using ABAQUS. An interpenetrating three-phase composite made of 420 stainless steel, 150P bronze and alumina are taken as an example. The elastic constants of the phases are given in Table I. The stainless steel is regarded as the matrix. The periodic displacement boundary conditions are prescribed on the unit cell, which are divided into 8000 linear eight-noded brick elements. For two given values 21.6% and 35.2% of the volume fraction of the steel phase, the effective Young's modulus E and shear modulus G of such a three-phase composite are plotted in Figure 7 as a function of the volume fraction of alumina. It is found again that the analytical results have a good agreement with the numerical solutions.

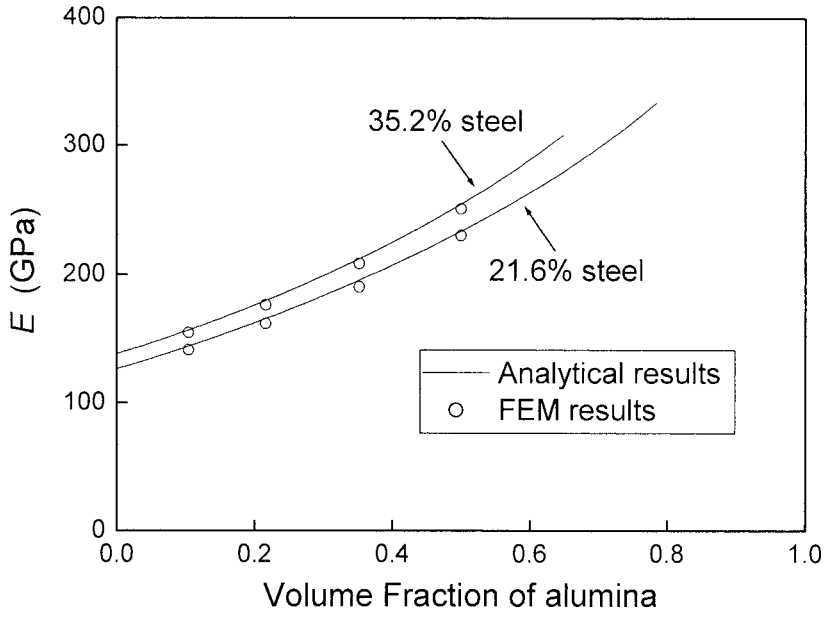

(a)

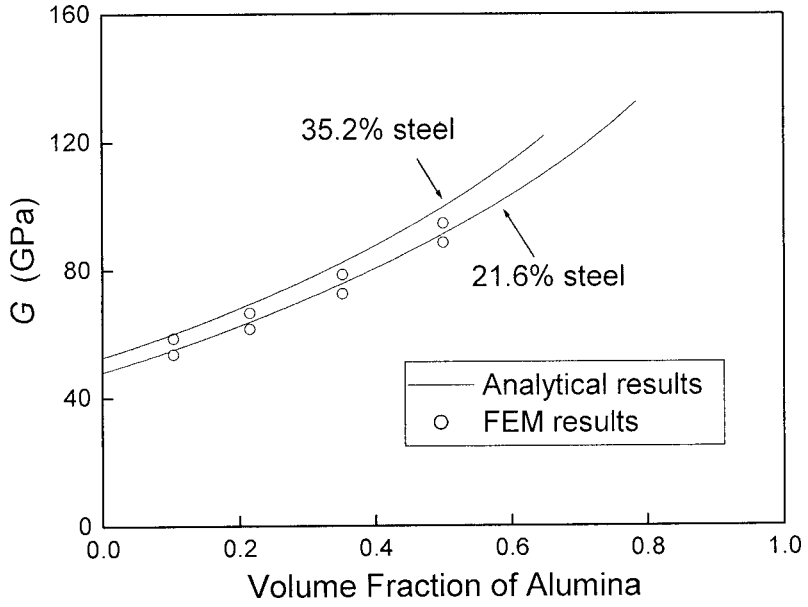

(b)

Figure 7. Effective elastic moduli of the interpenetrating stainless steel/bronze/alumina composite: (a) Young's modulus, and (b) shear modulus.

Table II. Volume fractions and elastic moduli of phases in a four-phase composite [9].

Phase number α	Phase material	Volume fraction f_α	Bulk modulus K_α (GPa)	Shear modulus G_α (GPa)
1	Al	0.16	67.6	25.9
2	B_4C	0.66	226.0	192.0
3	$A1B_2$	0.02	170.0	120.0
4	$A1_4BC$	0.16	175.0	129.0

4.4. EXAMPLE 4: A FOUR-PHASE COMPOSITE WITH TWO SELF-CONNECTED PHASES

A four-phase composite synthesized by Torquato and co-workers [9] is analyzed further, in which the B_4C and Al phases are self-connected in three-dimensions and the AlB_2 and Al_4BC phases exist in the form of dispersed inclusions. The elastic properties and volume fractions of the four phases are given by Torquato *et al.* [9] and, for completeness, are listed in Table II.

The B_4C phase is chosen as the self-connected matrix. According to the two-step calculation procedure, the effective moduli of the composite matrix comprising of the B_4C, AlB_2 and Al_4BC phase are first determined from the Mori–Tanaka method. Its Young's modulus and shear modulus are determined as $E_m = 414.72$ GPa and $G_m = 176.19$ GPa. Using the relation $f_1 = 3a^2 - 2a^3$ and the volume fraction of Al $f_1 = 0.16$, the parameter a equals to 0.2533. Then, the effective bulk modulus and shear modulus are derived from Equation (12) as $K = 169.9$ GPa and $G = 126.8$ GPa, which agree well with the experimental data of Torquato *et al.* [9], $K = 176$ GPa and $G = 125$ GPa.

5. Elastoplastic Constitutive Relation

5.1. THEORETICAL DERIVATION OF ELASTOPLASTIC RELATION

It is of great interest both in theoretical investigation and engineering application to predict the elastoplastic response of composites from the microstructures and the properties of the constituent phases. However, this non-linear problem is much more difficult than the estimation of effective elastic moduli. Micromechanical investigations on determination of elastoplastic stress-strain relations of composites are very limited as yet [28–31], especially for interpenetrating phase composites [32].

The unit cell model presented in Section 2 is now extended to calculate the plastic properties of interpenetrating phase composites. Due to the heterogeneous and non-linear features of plastic deformation, the stress-strain relation of a composite can only be obtained from the unit cell by using the step-by-step homogenization

scheme. A complete elastoplastic stress-strain relation can be obtained from the following steps:

(1) Calculate first the effective elastic moduli of the composite in the stage of elasticity when the applied strain loading is small, as described in Section 3;
(2) Calculate the stress distribution in the unit cell as a function of the applied displacement loading by using the iso-strain and iso-stress assumptions;
(3) Determine which sub-cell (say the kth one) will undergo plastic yielding next;
(4) Derive the effective stress-strain relation by using the homogenization method based on the sub-cell decomposition, analogously to the method in Section 4 except that the elastoplastic constitutive relations of the yielded sub-cells are employed;
(5) Repeat steps 2–4 until all the sub-cells undergo plastic deformation.

The above approach is now illustrated by a co-continuous two-phase composite (Figure 4). Assume that the matrix and the reinforcing phase obey the following elastoplastic constitutive relations with strain-hardening:

$$\begin{aligned} \frac{\varepsilon_{\mathrm{m}}}{\varepsilon_{\mathrm{m}}^{\mathrm{s}}} &= \begin{cases} \sigma_{\mathrm{m}}/\sigma_{\mathrm{m}}^{\mathrm{s}} & \text{for } \sigma_{\mathrm{m}} < \sigma_{\mathrm{m}}^{\mathrm{s}}, \\ (\sigma_{\mathrm{m}}/\sigma_{\mathrm{m}}^{\mathrm{s}})^{n_{\mathrm{m}}} & \text{for } \sigma_{\mathrm{m}} \geqslant \sigma_{\mathrm{m}}^{\mathrm{s}}, \end{cases} \\ \frac{\varepsilon_{\mathrm{r}}}{\varepsilon_{\mathrm{r}}^{\mathrm{s}}} &= \begin{cases} \sigma_{\mathrm{r}}/\sigma_{\mathrm{r}}^{\mathrm{s}} & \text{for } \sigma_{\mathrm{r}} < \sigma_{\mathrm{r}}^{\mathrm{s}}, \\ (\sigma_{\mathrm{r}}/\sigma_{\mathrm{r}}^{\mathrm{s}})^{n_{\mathrm{r}}} & \text{for } \sigma_{\mathrm{r}} \geqslant \sigma_{\mathrm{r}}^{\mathrm{s}}, \end{cases} \end{aligned} \tag{14}$$

where $\sigma_{\mathrm{m}}^{\mathrm{s}}$ and $\sigma_{\mathrm{r}}^{\mathrm{s}}$ denote the yield stresses of the matrix and the reinforcing phase, respectively, $\varepsilon_{\mathrm{m}}^{\mathrm{s}} = \sigma_{\mathrm{m}}^{\mathrm{s}}/E_{\mathrm{m}}$ and $\varepsilon_{\mathrm{r}}^{\mathrm{s}} = \sigma_{\mathrm{r}}^{\mathrm{s}}/E_{\mathrm{r}}$ the corresponding yield strains, n_{m} and n_{r} the strain-hardening exponents. When $n_{\mathrm{m}} = n_{\mathrm{r}} = 0$, the constitutive relations in Equation (14) correspond to elastic-perfectly plastic phases.

Assume that the composite is subjected to uniaxial tension in the x_3-axis direction. We consider this simple case for two reasons. First, the three-dimensional constitutive relation of an isotropic material can be extended from the stress-strain relation of uniaxial tension, as will be shown below. In other words, its independent elastic constants can generally be determined from the analysis of uniaxial tension. Second, the derivation in what follows for uniaxial tension can be generalized to other loading situations. As discussed in Section 3, the linear displacement boundary condition corresponding to the uniaxial tensile strain ε is prescribed on the unit cell. In addition, without loss of generality, we assume that the yield stress of the matrix is lower than that of the reinforcing phase, i.e., $\sigma_{\mathrm{m}}^{\mathrm{s}} < \sigma_{\mathrm{r}}^{\mathrm{s}}$.

With the increase in the tensile loading, the deformation of the unit cell in Figure 4(a) includes the following five regimes:

(1) In the first stage, all the sub-cells are elastic, and the composite undergoes only elastic deformation. From the iso-strain and iso-stress assumptions, the average stresses in the sub-cells are

$$\sigma_1 = E_{\mathrm{r}}\varepsilon, \qquad \sigma_2 = \sigma_3 = \varepsilon\left(\frac{a}{E_{\mathrm{r}}} + \frac{1-a}{E_{\mathrm{m}}}\right)^{-1}, \qquad \sigma_4 = E_{\mathrm{m}}\varepsilon, \tag{15}$$

where σ_k ($k = 1, \ldots, 4$) denotes the average stress in the kth sub-cell (Figure 4(b)). Then the homogenization method leads to the elastic stress-strain relation as

$$\sigma = \left[a^2 E_{\mathrm{r}} + (1-a)^2 E_{\mathrm{m}} + 2a(1-a)\left(\frac{a}{E_{\mathrm{r}}} + \frac{1-a}{E_{\mathrm{m}}}\right)^{-1}\right]\varepsilon. \tag{16}$$

(2) In the second stage, assume that the matrix in sub-cells 2 and 3 in Figure 4(b) has plastic deformation while all other materials are elastic. For different combination of material parameters, it is also possible that other sub-cells yield first, but the analysis method is similar. The average stresses in the sub-cells are given by

$$\sigma_1 = E_{\mathrm{r}}\varepsilon, \qquad \varepsilon = (1-a)\varepsilon_{\mathrm{m}}^{\mathrm{s}}\left(\frac{\sigma_2}{\sigma_{\mathrm{m}}^{\mathrm{s}}}\right)^{n_{\mathrm{m}}} + \frac{\sigma_2 a}{E_{\mathrm{r}}}, \qquad \sigma_4 = E_{\mathrm{m}}\varepsilon. \tag{17}$$

Then, the stress σ-strain ε relation in the second regime is obtained as

$$\sigma = [a^2 E_{\mathrm{r}} + (1-a)^2 E_{\mathrm{m}}]\varepsilon + 2a(1-a)\sigma_2, \tag{18}$$

where σ_2 is related to the applied strain ε by the second equation in (17).

(3) In the third stage, the matrix in sub-cells 2–4 in Figure 4(b) experiences plastic deformation while the reinforcing phase is elastic. The stress-strain relation in this stage can be obtained similarly as

$$\sigma = a^2 E_{\mathrm{r}}\varepsilon + 2a(1-a)\sigma_2 + (1-a)^2\sigma_{\mathrm{m}}^{\mathrm{s}}\left(\frac{\varepsilon}{\varepsilon_{\mathrm{m}}^{\mathrm{s}}}\right)^{\frac{1}{n_{\mathrm{m}}}}, \tag{19}$$

where σ_2 is related to the applied strain ε also by the second equation in (17).

(4) In the fourth stage, the reinforcing phase in sub-cells 2 and 3 is elastic while all the other parts undergo plastic deformation. The stress-strain relation is expressed as

$$\sigma = 2a(1-a)\sigma_2 + a^2\sigma_{\mathrm{r}}^{\mathrm{s}}\left(\frac{\varepsilon}{\varepsilon_{\mathrm{r}}^{\mathrm{s}}}\right)^{\frac{1}{n_{\mathrm{r}}}} + (1-a)^2\sigma_{\mathrm{m}}^{\mathrm{s}}\left(\frac{\varepsilon}{\varepsilon_{\mathrm{m}}^{\mathrm{s}}}\right)^{\frac{1}{n_{\mathrm{m}}}}, \tag{20}$$

where σ_2 is given also by the second equation in (17).

(5) In the final stage, all the blocks in the unit-cell undergo plastic deformation. The stress-strain relation is also given by Equation (20), except that σ_2 is related to ε by

$$\varepsilon = (1-a)\varepsilon_{\mathrm{m}}^{\mathrm{s}}\left(\frac{\sigma_2}{\sigma_{\mathrm{m}}^{\mathrm{s}}}\right)^{n_{\mathrm{m}}} + a\varepsilon_{\mathrm{r}}^{\mathrm{s}}\left(\frac{\sigma_2}{\sigma_{\mathrm{r}}^{\mathrm{s}}}\right)^{n_{\mathrm{r}}}. \tag{21}$$

Thus, the elastoplastic constitutive relation of an interpenetrating binary composite under tension is expressed analytically by Equations (16–21). For easier application, the above constitutive relation including five stages can be fitted by an elastic-power law hardening one:

$$\frac{\varepsilon}{\varepsilon_{\mathrm{s}}} = \begin{cases} \sigma/\sigma_{\mathrm{s}} & \text{for } \sigma < \sigma_{\mathrm{s}}, \\ (\sigma/\sigma_{\mathrm{s}})^n & \text{for } \sigma \geqslant \sigma_{\mathrm{s}}, \end{cases} \tag{22}$$

where σ_s and ε_s denote the yield stress and yield strain of the composite. Using the associated flow rule and the von Mises yield criterion, Equation (22) can be extended easily to the three-dimensional constitutive equation of the composite as

$$\frac{\varepsilon_{ij}}{\varepsilon_s} = \begin{cases} \dfrac{1+\nu}{E}\dfrac{\sigma_{ij}}{\sigma_s} - \dfrac{\nu}{E}\dfrac{\sigma_{kk}}{\sigma_s}\delta_{ij} & \text{for } \sigma_{eq} < \sigma_s, \\ \dfrac{3}{2}\left(\dfrac{\sigma_{eq}}{\sigma_s}\right)^{n-1}\dfrac{\sigma'_{ij}}{\sigma_s} & \text{for } \sigma_{eq} \geqslant \sigma_s, \end{cases} \tag{23}$$

where $\sigma'_{ij} = \sigma_{ij} - \frac{1}{3}\sigma_{kk}\delta_{ij}$ is the deviatoric stress tensor, and $\sigma_{eq} = (\frac{3}{2}\sigma'_{ij}\sigma'_{ij})^2$ the von Mises equivalent stress.

5.2. EXAMPLE

We take again the bi-continuous stainless steel/bronze composite as an example. The stress-strain relations of 420 stainless steel and 150P bronze under uniaxial tension are shown in Figures 8 and 9, respectively. By fitting these two curves, the yield stresses and strain-hardening exponents of the two phases are listed in Table I. The analytical solution in Equations (16–21), the numerical results of finite element method and the experimental results of Wegner and Gibson [2] for the stress-strain relation of the composite are compared in Figure 10. They coincide well with each other.

Then, the above theoretical solution including five stages is fitted into an elastic-power law strain-hardening curve in Equation (22) and extended to the three-dimensional elastoplastic constitutive relation in the form of Equation (23), where

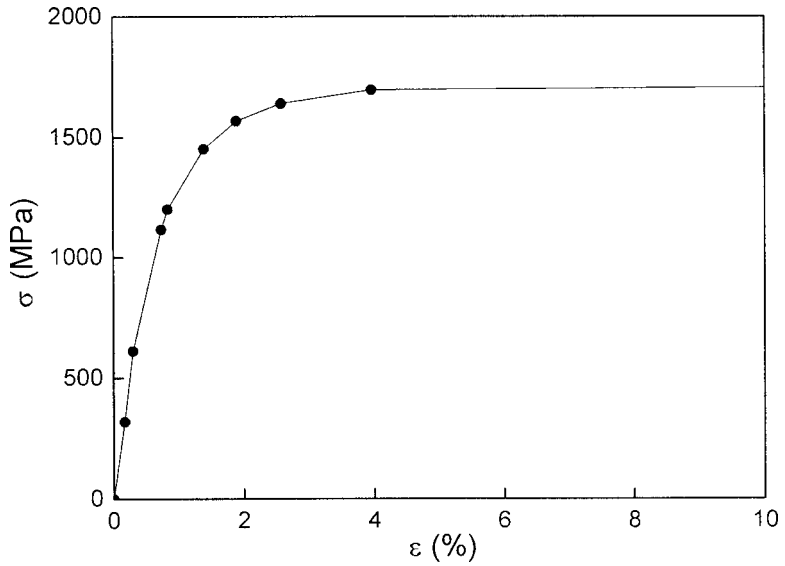

Figure 8. Stress-strain relation of 420 stainless steel under uniaxial tension.

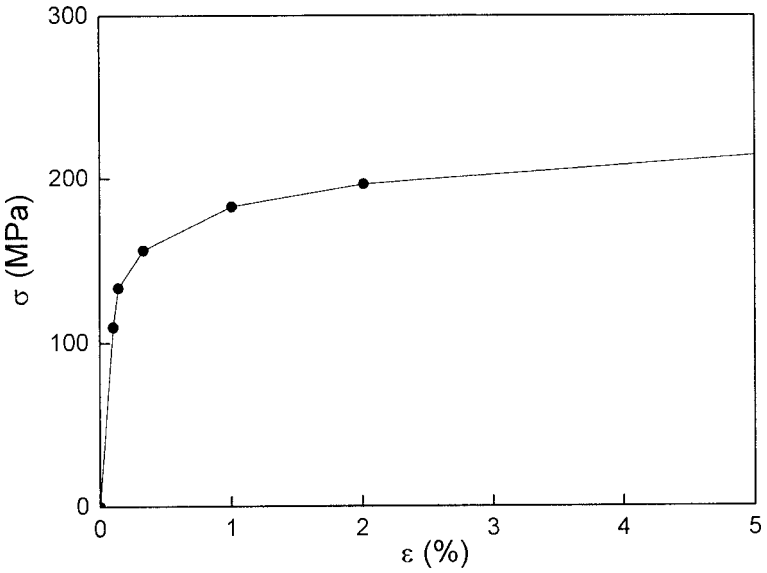

Figure 9. Stress-strain relation of 150P bronze under uniaxial tension.

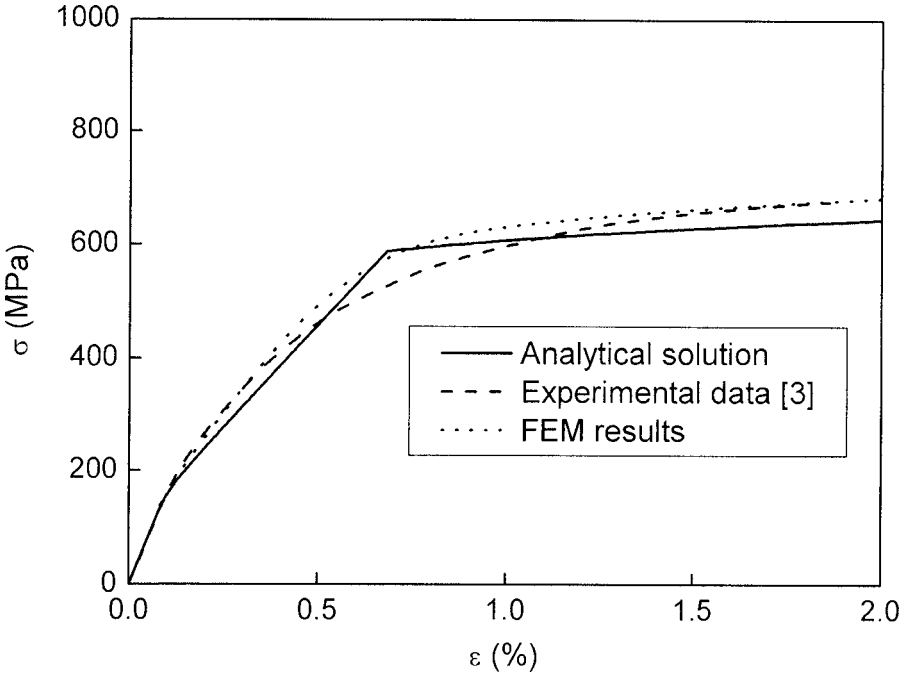

Figure 10. Stress-strain relation of bi-continuous stainless steel/bronze composite under uniaxial tension.

the material parameters are $\sigma_s = 244.5$ MPa, $\varepsilon_s = 0.0015$, and $n = 2.256$. It is seen that the micromechanical unit cell model presented in this paper is valid not only for estimating the effective elastic moduli but also for determining the elastoplastic constitutive relations for interpenetrating multiphase composites.

6. Conclusions

The mechanical properties of composites, e.g., stiffness, strength, toughness, thermal expansion and conductivity, depend not only on the volume fractions but also, to different extents, on the spatial distribution of the constituents and topological microsructure. The effective elastic moduli of interpenetrating phase composites cannot be obtained directly from the Eshelby's tensor, which constructs a basis of the conventional micromechanics of composites, because an interpenetrating network phase cannot be extracted as dispersed inclusions. In terms of the concept of connectivity developed by Newnham *et al.* [23], a cell model is presented in this work to determine the overall effective properties of composites reinforced with either dispersed inclusions or interpenetrating networks. The Mori–Tanaka method and the iso-stress and iso-strain assumptions are employed in an appropriate manner of combination, rendering the calculation of effective moduli quite easy and accurate. Via a step-by-step analysis of the unit cell, the three-dimensional strain-hardening elastoplastic constitutive relation can be derived. Such an approach should be of theoretical and engineering interest due to its simplicity and satisfactory accuracy. Though the attention of this work is focused mainly on the effective elastic moduli and elastoplastic constitutive relations of composites, the present micromechanics model can also be used to estimate other effective transport properties, such as thermal expansion and conductivity coefficients, piezoelectric and dielectric moduli of piezoelectric composites with interpenetrating microstructures.

Acknowledgments

We are grateful for support from the National Natural Science Foundation (Grant Nr. 10102008) and the Education Ministry of China (Grant Nr. 199926).

References

1. Clark, D. R., 'Interpenetrating Phase Composites', *Journal of the American Ceramic Society* **75**, 1992, 739–759.
2. Wegner, L. D. and Gibson, L. J., 'The Mechanical Behavior of Interpenetrating Phase Composites – I: Modelling', *International Journal of Mechanical Science* **42**, 2000, 925–942.
3. Wegner, L. D. and Gibson, L. J., 'The Mechanical Behaviour of Interpenetrating Phase Composites, II: A Case Study of a Three-Dimensionally Printed Material', *International Journal of Mechanical Science* **42**, 2000, 943–964.

4. Wegner, L. D. and Gibson, L. J., 'The Mechanical Behaviour of Interpenetrating Phase Composites, III: Resin-Impregnated Porous Stainless Steel', *International Journal of Mechanical Science* **43**, 2001, 1061–1072.
5. Liu, W. and Köster, U., 'Microstructures and Properties of Interpenetrating Alumina/Aluminium Composites Made by Reaction of SiO_2 Glass Preforms with Molten Aluminum', *Materials Science and Engineering* **A210**, 1996, 1–7.
6. Prielipp, H., Knechtel, M., Claussen, N., Streiffer, S. K., Müllejans, H., RüKhle, M. and Rödel, J., 'Strength and Fracture Toughness of Aluminum/Alumina Composites with Interpenetrating Networks', *Materials Science and Engineering* **A197**, 1995, 19–30.
7. Rödel, J., Prielipp, H., Claussen, N., Sternitzke, M., Alexander, K. B., Becher, P. F. and Schneibel, J. H., 'Ni_3Al/Al_2O_3 Composites with Interpenetrating Networks', *Scripta Metallurgica et Materialia* **33**, 1995, 843–848.
8. Skirl, S., Hoffman, M., Bowman, K., Wiederhorn, S. and Rödel, J., 'Thermal Expansion Behavior and Macrostrain of Al_2O_3/Al Composites with Interpenetrating Networks', *Acta Materialia* **46**, 1998, 2493–2499.
9. Torquato, S., Young, C. L. Y., Rintoul, M. D., Milius, D. L. and Aksay, I. A., 'Elastic Properties and Structure of Interpenetrating Boron Carbide/Aluminum Multiphase Composites', *Journal of the American Ceramic Society* **82**, 1999, 1263–1268.
10. Daehn, G. S., Starck, B., Xu, L., Elfishawy, K. F., Ringnalda, J. and Fraser, H. L., 'Elastic and Plastic Behavior of a Co-Continuous Aluminum/Alumina Composite', *Acta Materialia* **44**, 1996, 249–261.
11. Ravichandran, K. S., 'Deformation Behavior of Interpenetrating Phase Composites', *Composites Science and Technology* **52**, 1994, 541–549.
12. Peng, H. X., Fan, Z. and Evans, J. R. G., 'Bi-Continuous Metal Matrix Composites', *Materials Science and Engineering* **A303**, 2001, 37–45.
13. Aldrich, D. E. and Fan, Z., 'Microstructural Characterisation of Interpenetrating Nickel/Alumina Composites', *Materials Characterization* **47**, 2001, 167–173.
14. Aboudi, J., *Mechanics of Composite Materials: A Unified Micromechanical Method*, Elsevier, Amsterdam, 1991.
15. Nemat-Nasser, S. and Hori, M., *Micromechanics: Overall Properties of Heterogeneous Materials*, North-Holland, Amsterdam, 1993.
16. Torquato, S., *Random Heterogeneous Materials: Microstructure and Macroscopic Properties*, Springer, Heidelberg, 2002.
17. Poech, M. H. and Ruhr, D., 'Die quantitative Charakterisierung der Gefügeanordnung', *Praktische Metallographie Sonderband* **324**, 1999, 385–391.
18. Lessle, P., Dong, M., Soppa, E. and Schmauder, S., 'Simulation of Interpenetrating Microstructures by Self-Consistent Matricity Models', *Scripta Materialia* **38**, 1998, 1327–1332.
19. Dong, M., Soppa, E. and Schmauder, S., 'Modelling of Metal Matrix Composites by a Self-Consistent Embedded Cell Model', *Acta Materialia* **44**, 1996, 2465–2478.
20. Levassort, R., Lethiecq, M., Desmare, R. and Tran-Huu-Hue, L. P., 'Effective Electroelastic Moduli of 3-3(0-3) Piezocomposites', *IEEE Transactions on Ultrasonics, Ferroelectrics, and Frequency Control* **46**, 1999, 1028–1034.
21. Torquato, S., 'Random Heterogeneous Media: Microstructure and Improved Bounds on the Effective Properties', *Applied Mechanics Review* **44**, 1991, 37–76.
22. Torquato, S. 'Modeling of Physical Properties of Composite Materials', *International Journal of Solids and Structures* **37**, 2000, 411–422.
23. Newnham, R. E., Skinner, D. P. and Cross, L. E., 'Connectivity and Piezoelectric-Pyroelectric Scheme', *Materials Research Bulletin* **13**, 1978, 525–536.
24. Peng, H. X., Fan, Z. and Evans, J. R. G., 'Factors Affecting the Microstructure of a Fine Ceramic Foam', *Ceramic International* **26**, 2000, 887–895.

25. Mori, T. and Tanaka, K., 'Average Stress in Matrix and Average Elastic Energy of Materials with Misfitting Inclusions', *Acta Metallurgica* **21**, 1973, 571–583.
26. Walpole, L. J., 'On the Overall Elastic Moduli of Composite Materials', *Journal of the Mechanics and Physics of Solids* **17**, 1969, 235–251.
27. Mura, T., *Micromechanics of Defects in Solids*, Martinus Nijhoff Publishers, The Netherlands, 1987.
28. Michel, J. C., Moulinec, H. and Suquet, P., 'Effective Properties of Composite Material with Periodic Microstructure: A Computational Approach', *Computational Methods in Applied Mechanics and Engineering* **172**, 1999, 109–143.
29. Ponte Castañeda, P. and Suquet, P., 'Nonlinear Composites', *Advances in Applied Mechanics* **34**, 1998, 171–302.
30. Teply, J. L. and Dvorak, G. J., 'Bounds on Overall Instantaneous Properties of Elastic-Plastic Composites', *Journal of the Mechanics and Physics of Solids* **36**, 1988, 29–58.
31. Hu, G. K., 'A Method of Plasticity for General Aligned Spheroidal Void or Fiber-Reinforced Composites', *International Journal of Plasticity* **12**, 1996, 439–449.
32. Gonzalez, C. and LLorca, J., 'A Self-Consistent Approach to the Elastoplastic Behaviour of Two-Phase Materials Including Damage', *Journal of the Mechanics and Physics of Solids* **48**, 2000, 675–692.